

# Magnetized strange quark matter in a mass-density-dependent model<sup>\*</sup>

HOU Jia-Xun(侯佳荀)<sup>1</sup> PENG Guang-Xiong(彭光雄)<sup>1,2</sup> XIA Cheng-Jun(夏铖君)<sup>2</sup> XU Jian-Feng(徐建峰)<sup>2;1)</sup>

<sup>1</sup> Theor. Physics Center for Science Facilities, Institute of High Energy Physics,  
Chinese Academy of Sciences, Beijing 100049, China

<sup>2</sup> School of Physics, University of Chinese Academy of Sciences, Beijing 100049, China

**Abstract:** We investigate the properties of strange quark matter (SQM) in a strong magnetic field with quark confinement by the density dependence of quark masses considering the total baryon number conservation, charge neutrality and chemical equilibrium. It is found that an additional term should appear in the pressure expression to maintain thermodynamic consistency. At fixed density, the energy density of magnetized SQM varies with the magnetic field strength. By increasing the field strength an energy minimum exists located at about  $6 \times 10^{19}$  Gauss when the density is fixed at two times the normal nuclear saturation density.

**Key words:** quark matter, thermodynamic consistency, mass-density dependence, strange stars

**PACS:** 24.85.+p, 12.38.MH, 25.75.-q **DOI:** 10.1088/1674-1137/39/1/015101

## 1 Introduction

Strange quark matter (SQM) is a new form of matter that contains a large number of deconfined quarks in  $\beta$ -equilibrium, with electric and color charge neutrality. After Witten conjectured that SQM could be the true ground state of strong interactions [1–3], Farhi and Jaffe [4] studied SQM in the framework of the MIT bag model [5] with various values of the strange quark mass and the bag constant. SQM could be found in the inner core of a neutron star where strange quarks would be produced through the weak processes with dynamic chemical equilibrium among the constituents. It is possible that after a supernova explosion its core directly forms a strange quark star (SQS) [6, 7]. An astrophysical object could also form a hybrid star that has a quark core and a crust of hadronic matter.

The stability of SQM is strongly affected in a strong magnetic field [8]. The typical strength on the surface of pulsars could be of the order  $\sim 10^{12}$  G. Magnetars and neutron stars could be associated with sources with intense magnetic fields around  $\sim 10^{13}$ – $10^{15}$  G or even higher [9, 10]. The origin of such ultrastrong magnetic fields could be explained in two ways. One is the magnetohydrodynamic dynamo mechanism with large magnetic fields generated by rotating plasma of a protoneutron star [10]. The other is that during the star collapse with magnetic flux conservation, the relatively small magnetic fields were amplified [11]. In recent research, it was found that noncentral high-energy heavy-ion col-

lisions could generate intense magnetic fields as high as about  $10^{19}$  G, corresponding to  $eB_m \sim 6m_\pi^2$ , where  $e$  is the fundamental electric charge and  $m_\pi$  is the pion mass.

Since the lattice approach still has difficulty in consistent treatment of the finite chemical potential, and the application of perturbative quantum chromodynamics (QCD) to the strong-coupling domain is unbelievable, one has to use phenomenological models in most cases. In Ref. [8], Chakrabarty studied quark matter in a strong magnetic field with the conventional MIT bag model, and found that SQM becomes more stable if the order of the strength of the magnetic field is greater than some critical value. In Refs. [12, 13], the authors confirmed that there is an anisotropy of pressures due to the strong magnetic field [14–16] and that the MIT bag model can be used to study magnetized SQM (mSQM) satisfactorily. With the Nambu-Jona-Lasinio (NJL) model the properties of mSQM were also discussed by many researchers [17–21]. The linear sigma model coupled to quarks and to the Polyakov loop was also used to investigate the influence of a strong magnetic field on confinement and chiral properties of QCD [22].

It is well known that particle masses vary with environment. Such masses are usually called effective masses [23–26]. Effective masses and effective bag constants for quark matter have been broadly studied [27, 28]. For example, in a quasiparticle model, the particle mass is derived at the zero-momentum limit of the dispersion relations from an effective quark propagator by resumming one-loop self-energy diagrams in the hard-dense-loop

Received 7 March 2014, Revised 14 April 2014

<sup>\*</sup> Supported by National Natural Science Foundation of China (11135011, 11475110) and CAS Key Project (KJCX3-SYW-N2)

1) E-mail: xjfil@126.com

©2015 Chinese Physical Society and the Institute of High Energy Physics of the Chinese Academy of Sciences and the Institute of Modern Physics of the Chinese Academy of Sciences and IOP Publishing Ltd

approximation. This reveals the dependence of particle masses on chemical potentials. In recent research [29], the authors extended the quasiparticle model to studying mSQM. They found a density- and magnetic-field-dependent bag function, which has a maximum at 2–3 times the saturation density when the QCD scale parameter is larger than 123 MeV.

In the present paper, we apply another quark model with confinement by the density dependence of quark masses (QMDD). In this model the masses of quarks depend upon the baryon number density. This idea was initially introduced by Fowler, Raha, and Weiner to study light quark matter [30]. Later Chakrabarty and co-workers applied the model to the case of SQM [31–33]. The main advantage of QMDD is the inclusion of quark confinement without using the bag constant. Instead, it is achieved by the density dependence of the quark masses derived from in-medium chiral condensates [34–36]. The two most important aspects in this model are the quark mass scaling and the thermodynamic treatment. Originally, the interaction part of the quark masses was assumed to be inversely proportional to the density [30, 31]. Researchers also suggested other mass scalings [37, 38]. In Ref. [34] and [36], a cubic root scaling was derived based on the in-medium chiral condensates and linear confinement at zero and finite temperature respectively. This scaling has been used to investigate many aspects of SQM [39–42]. In the present article, we use the QMDD model with cubic root mass scaling to study the properties of SQM in a strong magnetic field.

The paper is organized as follows. In Section 2, we derive the thermodynamic formulas when quark masses are density dependent. In Section 3, we analyze the properties of mSQM and present our numerical results. In Section 4, the mass-radius relation of magnetized quark stars is investigated. A short summary is presented in Section 5.

## 2 Thermodynamic treatment

In the QMDD model, quark confinement is achieved by the density dependence of quark masses: with decreasing density, the mass of a quark becomes infinitely large so that the vacuum is unable to support it. Therefore, the proper form of the density dependence is very important. Originally, the quark masses are parameterized as

$$m_q = m_{q0} + \frac{B}{3n}, \quad (1)$$

where  $q=u, d, s$  quarks,  $m_{q0}$  is the current mass of quark flavor  $q$ ,  $B$  is the famous MIT bag constant,  $n$  is the baryon number density.

Based on the in-medium chiral condensates, a cubic root scaling was derived at zero temperature [34], and

extended to finite temperature [36]. We adopt this mass scaling in the present article. At zero temperature, the mass scaling is

$$m_q = m_{q0} + \frac{D}{n^{\frac{1}{3}}}, \quad (2)$$

where  $m_{q0}$  is the quark current mass,  $D$  is the confinement parameter,  $n$  is the total baryon number density, the exponent of density was derived based on the in-medium chiral condensates and linear confinement at zero temperature [34]. In the present model, the parameters are quark current masses  $m_{u0}$ ,  $m_{d0}$ ,  $m_{s0}$ , and the confinement parameter  $D$ . The electron does not participate in the strong interaction; its mass is a constant, i.e.  $m_e = 0.511$  MeV. Since the light-quark current masses are too small compared to the interaction part, we take  $m_{u0} = m_{d0} = 0$ . The strange quark current mass is  $95 \pm 25$  MeV [43]. The parameter  $D$  has been discussed in Refs. [35, 36, 44]. We treat  $D$  as a free parameter here. The value of  $D^{1/2}$  should be in the range (156, 270) MeV [36, 44].

The starting point of our manipulation for SQM in a strong magnetic field is the energy density. Let us start with the energy density expression of a free particle system

$$E = \sum_i \frac{2g_i}{(2\pi)^3} \iiint \sqrt{p^2 + m_i^2} d^3\vec{p}, \quad (3)$$

where the summation goes over all particles involved,  $g_i$  is the degeneracy factor with  $g_i = 3$  (color) for quarks and  $g_i = 1$  for electrons. The degeneracy due to spin has been denoted by factor 2 in the numerator.

We assume the magnetic field to be directed along the  $z$  axis with constant field strength  $B_m$ . The single particle energy spectrum is given by [45]

$$\epsilon = \sqrt{p_z^2 + m_i^2 + e_i B_m (2l \pm 2s + 1)}, \quad (4)$$

where  $l=0, 1, 2, \dots$ , are the principal quantum numbers for Landau levels,  $e_i$  is the absolute value of the electronic charge,  $e_i = |q_i|$  (i.e.  $e_u = 2/3$ ,  $e_d = e_s = 1/3$ , and  $e_e = 1$ ),  $s = \pm 1/2$  refers to spin-up or spin-down states, and  $p_z$  is the component of particle momentum along the direction of the external magnetic field. The notation ‘ $\pm$ ’ is a plus or minus sign if the corresponding particles are negatively or positively charged. The anomalous moments of quarks and electrons are either small or not well understood and thus not considered here.

Setting  $\nu = l - \text{sign}(q_i)s + 1/2$ , the single particle energy spectrum becomes

$$\epsilon = \sqrt{p_z^2 + m_i^2 + 2\nu e_i B_m} \equiv \sqrt{p_z^2 + M_{i,\nu}^2}, \quad (5)$$

where we have used the definition

$$M_{i,\nu} \equiv \sqrt{m_i^2 + 2\nu e_i B_m}. \quad (6)$$

We now should replace the integration over  $p_x$ - $p_y$  plane in the momentum space by the rule [8]

$$2 \iint dp_x dp_y \rightarrow 2\pi e_i B_m \sum_{\nu} (2 - \delta_{\nu 0}). \quad (7)$$

Accordingly, the energy density for the  $i$ th ( $i=u, d, s$  and  $e$ ) species is given by

$$E_i = \frac{g_i e_i B_m}{4\pi^2} \sum_{\nu=0}^{\nu_{\max}} (2 - \delta_{\nu 0}) \times \int \sqrt{p_z^2 + m_i^2 + 2\nu e_i B_m} dp_z. \quad (8)$$

Explicitly carrying out the integration gives

$$E_i = \frac{g_i e_i B_m}{4\pi^2} \sum_{\nu=0}^{\nu_{\max}} (2 - \delta_{\nu 0}) \left[ \epsilon_i \sqrt{\epsilon_i^2 - M_{i,\nu}^2} + M_{i,\nu}^2 \ln \left( \frac{\epsilon_i + \sqrt{\epsilon_i^2 - M_{i,\nu}^2}}{M_{i,\nu}} \right) \right], \quad (9)$$

where  $\epsilon_i$  is the Fermi energy for particle type  $i$ ,  $p_{i,\nu} = \sqrt{\epsilon_i^2 - M_{i,\nu}^2}$  is the maximum value of  $p_z$  for the energy level  $\nu$ . From the positive value requirement on the Fermi energy we can determine the upper bound  $\nu_{\max}$  of the summation index  $\nu$

$$\nu \leq \nu_{\max} \equiv \text{int} \left[ \frac{\epsilon_i^2 - m_i^2}{2e_i B_m} \right], \quad (10)$$

where  $\text{int}[\ ]$  means taking the integer part.

In the presence of a magnetic field, according to the rule in Eq. (7), the expression of the number density can apparently be given as

$$\begin{aligned} n_i &= \frac{g_i e_i B_m}{2\pi^2} \sum_{\nu=0}^{\nu_{\max}} (2 - \delta_{\nu 0}) \int_0^{p_{i,\nu}} dp_z \\ &= \frac{g_i e_i B_m}{2\pi^2} \sum_{\nu=0}^{\nu_{\max}} (2 - \delta_{\nu 0}) \sqrt{\epsilon_i^2 - M_{i,\nu}^2}. \end{aligned} \quad (11)$$

The chemical potentials are connected to the energy density by

$$dE = \sum_i \mu_i dn_i, \quad (12)$$

where

$$dE = \sum_i dE_i = \sum_i \left( \frac{\partial E_i}{\partial \epsilon_i} d\epsilon_i + \frac{\partial E_i}{\partial m_i} dm_i \right), \quad (13)$$

$$dn_i = \frac{\partial n_i}{\partial \epsilon_i} d\epsilon_i + \frac{\partial n_i}{\partial m_i} dm_i, \quad (14)$$

$$dm_i = \sum_j \frac{\partial m_i}{\partial n_j} dn_j. \quad (15)$$

Using these relations, we finally have

$$\mu_i = \epsilon_i + \mu_l, \quad (16)$$

with

$$\begin{aligned} \mu_l &= -\frac{1}{3} \frac{dm_l}{dn} \sum_j \frac{g_j e_j m_j B_m}{2\pi^2} \sum_{\nu=0}^{\nu_{\max}} (2 - \delta_{\nu 0}) \\ &\quad \times \ln \left( \frac{\epsilon_j + \sqrt{\epsilon_j^2 - M_{j,\nu}^2}}{M_{j,\nu}} \right). \end{aligned} \quad (17)$$

Because all particle masses do not depend on the density of electrons, i.e.  $\frac{\partial m_i}{\partial n_e} = 0$ , the summation is just over  $u, d, s$  and the term  $\mu_l$  as a whole is independent of quark flavors.

In order to obtain the equation of states and check the thermodynamic consistency, we use the thermodynamic relation between pressure and the chemical potentials  $\mu_i$ :

$$P = -E + \sum_i \mu_i n_i, \quad (18)$$

which is valid for an arbitrary infinitely large system.

Substituting Eqs (9), (11), (16), (17) into equation (18) gives

$$P = -\Omega_0 + \delta P, \quad (19)$$

where  $\Omega_0$  is the free particle contribution, i.e.

$$\begin{aligned} \Omega_0 &= -\sum_i \frac{g_i e_i B_m}{4\pi^2} \sum_{\nu=0}^{\nu_{\max}} (2 - \delta_{\nu 0}) \\ &\quad \times \left\{ \epsilon_i (\epsilon_i^2 - M_{i,\nu}^2)^{1/2} \right. \\ &\quad \left. - M_{i,\nu}^2 \ln \left[ \frac{\epsilon_i + \sqrt{\epsilon_i^2 - M_{i,\nu}^2}}{M_{i,\nu}} \right] \right\}, \end{aligned} \quad (20)$$

and  $\delta P$  appears due to the density dependence of quark masses

$$\begin{aligned} \delta P &= -\frac{D}{3n^{1/3}} \sum_j \frac{g_j e_j m_j B_m}{2\pi^2} \sum_{\nu=0}^{\nu_{\max}} (2 - \delta_{\nu 0}) \\ &\quad \times \ln \left( \frac{\epsilon_j + \sqrt{\epsilon_j^2 - M_{j,\nu}^2}}{M_{j,\nu}} \right). \end{aligned} \quad (21)$$

### 3 Properties of mSQM

As usually done, we consider mSQM as a mixture of  $u, d, s$  quarks and electrons. The weak equilibrium condition gives

$$\mu_u + \mu_e = \mu_d, \quad (22)$$

$$\mu_d = \mu_s. \quad (23)$$

Considering Eq. (16), we have

$$\epsilon_u + \epsilon_e = \epsilon_d, \quad (24)$$

and

$$\epsilon_d = \epsilon_s. \quad (25)$$

The charge neutrality condition gives

$$\frac{2}{3} n_u - \frac{1}{3} n_d - \frac{1}{3} n_s - n_e = 0, \quad (26)$$

and the baryon number density is given by

$$n = \frac{1}{3}(n_u + n_d + n_s). \quad (27)$$

Equations (24)–(27), together with Eq. (11), form the full set of self-consistent equations for finding the Fermi energy for quarks and electrons. We solve these equations numerically at a given density  $n$  and for different values of  $B_m$ , and then evaluate the thermodynamical quantities of the mSQM system.

In Fig. 1, the energy per baryon of mSQM is shown as functions of the baryon number density for different parameter sets. For each parameter set the pressure is zero at the minimum of the energy per baryon. In fact from Eqs. (18), (12), (22) and (23) one can obtain

$$P = n^2 \frac{d(E/n)}{dn}. \quad (28)$$

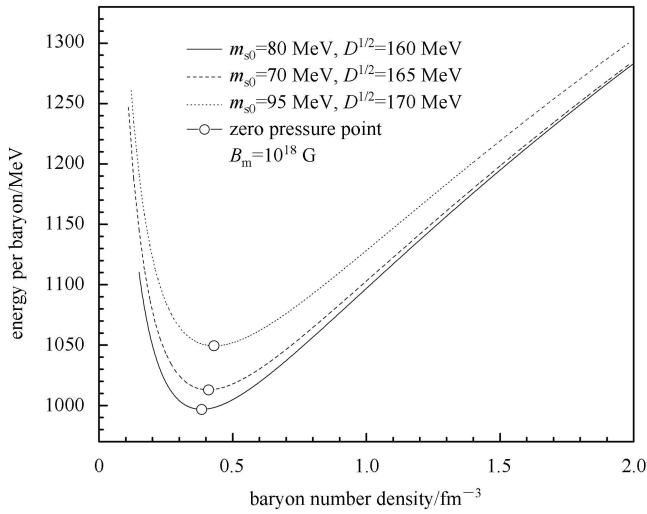


Fig. 1. Energy per baryon of mSQM in the present model. The energy minimum is located exactly at the same point of the zero pressure.

This relation must be satisfied for a fully thermodynamically consistent treatment. In the present paper, we assume the magnetic field to be directed along the  $z$  axis and is a constant. If one allows the magnetic field to vary with the density, one should add another new term to the chemical potential. The details of the magnetic field variation with the baryon number density is beyond this paper.

In Fig. 2, we plot the quark fractions, i.e.  $n_u/(3n)$ ,  $n_d/(3n)$ ,  $n_s/(3n)$ , and the  $10^3$  times the electron fraction,  $1000n_e/(3n)$ , versus the baryon number density for  $D^{1/2} = 160 \text{ MeV}$  and  $m_{s0} = 80 \text{ MeV}$ . The magnetic field strength is  $B_m = 10^{18} \text{ G}$ . The fraction of up quarks is always about one third. The fraction of down quarks decreases with increasing density while the fraction of strange quarks increases with increasing density. Both

fractions approach one third when the density is large enough. The figure indicates that the fraction of electrons is very small and it decreases with increasing density. The ladder-like shape is introduced by the quantized Landau levels. We can expect that when the density increases to a large enough value, the current mass of strange quarks can be ignored and all three kinds of quarks can be treated with equal footing. This is easy to understand. For fermions at zero temperature, the states below Fermi energy are all occupied. Adding particles into the system just enlarges the Fermi energy. At the same time the effective mass decreases with density. When the Fermi momentum is sufficiently large, the

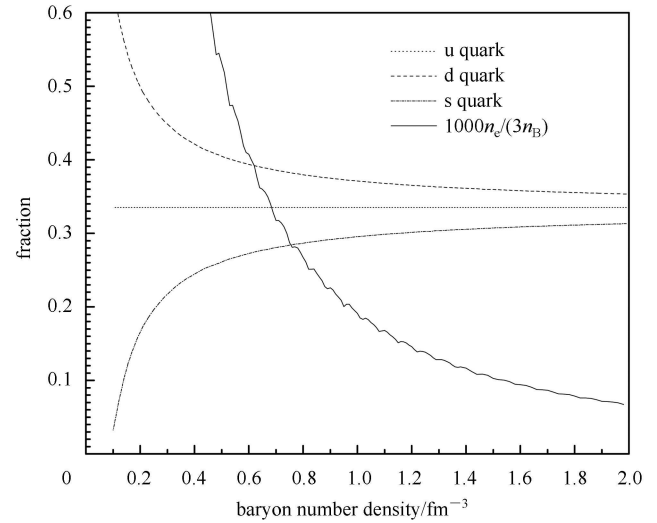


Fig. 2. Quark fraction versus baryon number density for  $D^{1/2} = 160 \text{ MeV}$ ,  $m_{s0} = 80 \text{ MeV}$  and  $B_m = 10^{18} \text{ G}$ .

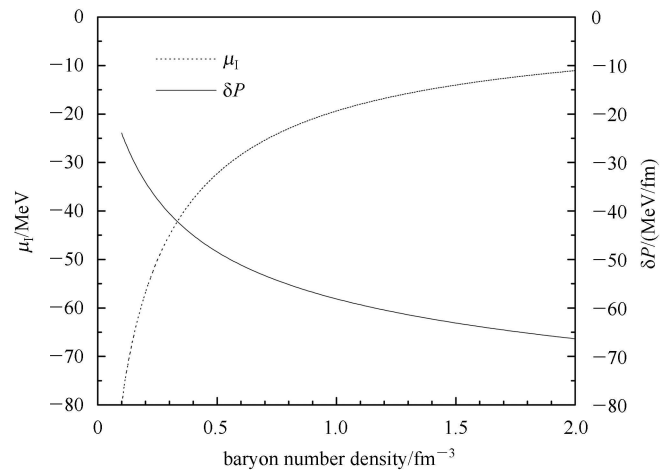


Fig. 3. The terms introduced by the density dependence of quark masses for pressure and chemical potential versus baryon number density.  $D^{1/2} = 160 \text{ MeV}$ ,  $m_{s0} = 80 \text{ MeV}$  and  $B_m = 10^{18} \text{ G}$ .

masses of most particles are ignorable compared to their momenta and we can treat them as if their effective masses are zero.

To explicitly demonstrate the properties of  $\mu_I$  and  $\delta P$ , we plot them in Fig. 3. The  $\mu_I$  term tends to reduce the total value, but the effects become gradually weaker when the baryon number density increases. For  $\delta P$ , it is a negative number and the curve shows an increasing tendency of the absolute value with baryon number density. However, its relative importance to the free particle contribution becomes smaller with increasing density.

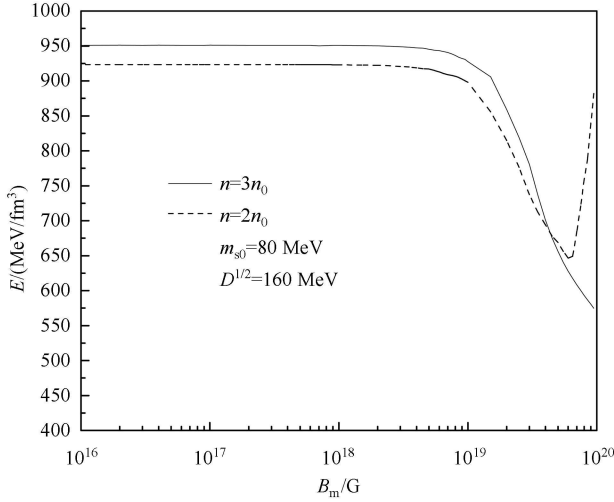


Fig. 4. Energy density of mSQM as a function of the magnetic field strength. The parameter pair  $(m_{s0}, D^{1/2})$  in MeV is  $(80, 160)$ . The solid line is for  $n = 3n_0$  and the dash line is for  $n = 2n_0$  ( $n_0 = 0.16 \text{ fm}^{-3}$ ).

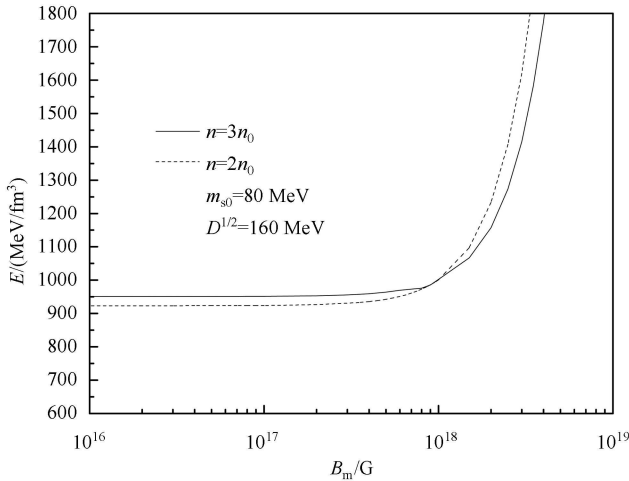


Fig. 5. Energy density plus that of the magnetic field as a function of the magnetic field strength. The parameter pair  $(m_{s0}, D^{1/2})$  in MeV is  $(80, 160)$ . The solid line is for  $n = 3n_0$  and the dash line is for  $n = 2n_0$  ( $n_0 = 0.16 \text{ fm}^{-3}$ ).

In Fig. 4, we show how the energy density of mSQM varies with the magnetic field strength at given densities  $n = 2n_0$  (dotted curve) and  $n = 3n_0$  (solid curve). For small  $B_m$ , it is very obvious that the energy density of mSQM is nearly constant. When the magnetic field strength exceeds a critical value, which is about  $3 \times 10^{18} \text{ G}$  for  $n = 2n_0$ , the energy density begins to decrease, until a minimum is reached. The minimum depends on the density. It is  $6 \times 10^{19} \text{ G}$  for  $n = 2n_0$ . If one includes the pure magnetic field term  $B_m^2/2$ , as shown in Fig. 5, the minimum disappears and the total energy density increases monotonously. This is because the magnetic field itself becomes dominant at extreme strong strength.

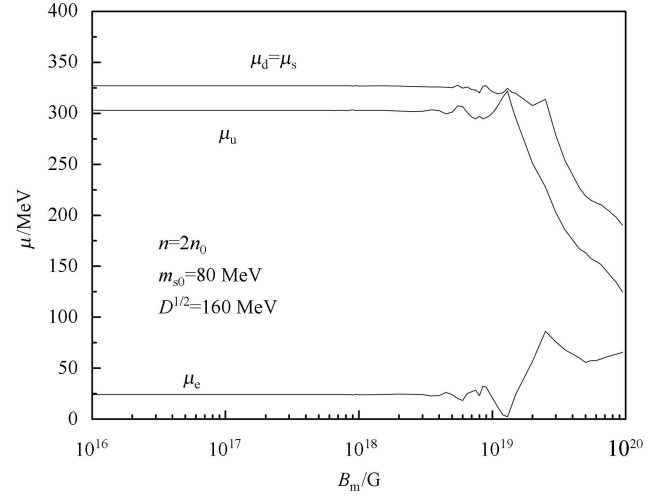


Fig. 6. Chemical potentials as a function of the magnetic field strength at zero temperature for  $n = 2n_0$ .

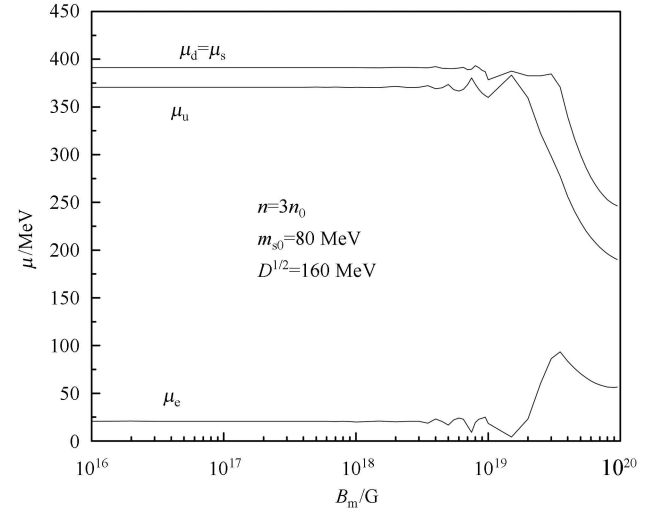


Fig. 7. Chemical potentials as a function of the magnetic field strength at zero temperature for  $n = 3n_0$ .

Figure 6 and Fig. 7 show the chemical potentials as functions of the magnetic field for  $n = 2n_0$  and  $n = 3n_0$  respectively. The chemical potentials keep approximately constant with the increasing magnetic field for  $B_m \leq 10^{18}$  G. The apparent Landau oscillation of chemical potentials appears between  $3 \times 10^{18} - 2 \times 10^{19}$  G. At  $B_m \geq 3 \times 10^{19}$  G quark chemical potentials decrease with magnetic field. We notice that in both figures the chemical potential of the electron dramatically climbs from an initial relatively small value to its summit (about 80 MeV) in the interval  $2 \times 10^{19} \text{ G} \leq B_m \leq 3 \times 10^{19} \text{ G}$ , then decreases to a relatively high and even stage (about 60 MeV). We have not encountered negative chemical potential for an electron.

In Fig. 8 we show the pressure as a function of the strength of the magnetic field for  $n = 3n_0$  (solid line) and  $n = 2n_0$  (dash line). At the beginning the pressure stays nearly constant and starts to decrease apparently at  $2 \times 10^{18}$  G.

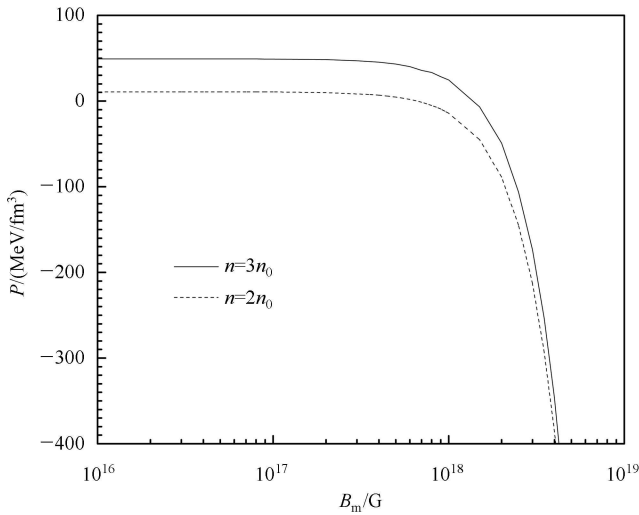


Fig. 8. Pressure in mSQM at zero temperature as a function of the magnetic field strength for  $m_{s0} = 80$  MeV and  $D^{1/2} = 160$  MeV.

#### 4 Mass-radius relation of magnetized SQSs

It has been speculated that the currently named neutron stars might in fact be SQSs [46], a family of compact stars consisting completely of deconfined u, d, s quarks. The structure of SQSs has attracted plenty of researchers. We now investigate the mass-radius relation of SQSs in ordinary phase in the framework of the new EOS we obtained in the preceding section. In principle, the pressure in mSQM is anisotropic [47, 48]. However, one presently does not exactly know at how high a density the difference between the longitudinal pressure  $p_l$  and the transverse pressure  $p_t$  becomes significant. We therefore work in the density region where  $p_l \approx p_t$ .

We numerically solve Toman-Oppenheimer-Volkoff (TOV) equations when fixing a central pressure  $P_c$ , and obtain a mass-radius relation by continuously varying the central pressure. For a concrete description of the solving process, one may refer to Ref. [35]. In fact, we alter the parameter  $D$  and magnetic field strength  $B_m$  to see how the magnetic field affects the structure of SQSs. The results have been shown in Fig. 9. The full dots represent the maximum mass on each line.

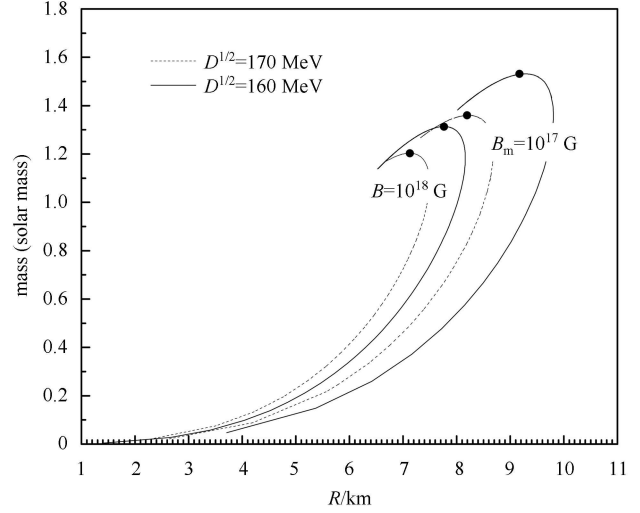


Fig. 9. The mass-radius relation of SQSs at different magnetic fields  $B_m$  with  $D^{1/2} = 160$  MeV (solid lines) and  $D^{1/2} = 170$  MeV (dash lines). The maximum masses on each curve are marked by full dots.

We can see that the larger  $B_m$  or  $D$  could produce a smaller maximum mass. According to Fig. 5 and Fig. 8, enhancing the magnetic field strength will increase energy density and decrease pressure which means a softer EOS. Therefore the present EOS is unable to produce the maximum star mass as large as two times the solar mass ( $2M_\odot$ ) [49, 50]. This is due to the fact that the quark mass scaling used in the present calculations includes only the confinement interaction effects whose contribution to the pressure is negative, while the perturbative interactions become important at high density. Therefore, it is meaningful to deduce a quark mass scaling considering both the confinement and perturbative effects [51], which is a forthcoming task in the near future.

#### 5 Summary

We have extended the QMDD model with a cubic root mass scaling to study the properties of SQM in the presence of a strong magnetic field. Our thermodynamic treatment automatically guarantees the self-consistency. It is found that at high density, quarks of different kinds

can be treated equivalently for dynamic properties and an individual particle acts like a free particle while the overall effect introduced by the density dependence of quark masses always exist. The magnetic field will reduce the energy density of pure magnetized SQM at a certain range of the field strength. At  $B_m \leq 10^{18}$  G, the magnetic field affects the properties of the system only slightly. At  $10^{18} \text{ G} \leq B_m \leq 10^{19} \text{ G}$ , Laudau oscillation appears in chemical potentials and the pressure dramati-

cally decreases. At  $B_m \approx 4 \times 10^{18}$  G the energy density of the pure magnetic field becomes comparable with, and finally much larger than that of the pure magnetized SQM. With the obtained EOS, we study the mass-radius relation of quark stars, and find that one cannot produce a pure quark star with a mass as large as  $2M_\odot$  considering only the confinement interaction in the cubic-root quark mass scaling. A quark mass scaling with both confinement and perturbative interactions is needed.

## References

- 1 Bodmer A R. Phys. Rev. D, 1971, **4**: 1601
- 2 Terazawa H. INS-Report 336, University of Tokyo. 1979
- 3 Witten E. Phys. Rev. D, 1984, **30**: 272
- 4 Farhi E, Jaffe R L. Phys. Rev. D, 1984, **30**: 2379
- 5 Chodos A, Jaffe R L, Johnson K, Thorn C B, Weiskopf V F. Phys. Rev. D, 1974, **9**: 3471
- 6 Hatsuda T. Mod. Phys. Lett. A, 1987, **2**: 805
- 7 Sato K, Suzuki H. Phys. Rev. Lett., 1987, **58**: 2722
- 8 Chakrabarty S. Phys. Rev. D, 1996, **54**: 1306
- 9 Duncan R, Thompson C. Astron. J., 1992, **32**: L9
- 10 Kouveliotou C et al. Nature, 1988, **393**: 235
- 11 Tatsumi T, Maruyama T, Nakano E, Nawa K. Nucl. Phys. A, 2006, **774**: 827
- 12 Martínez A Pérez, Pérez Rojas H, Mosquera Cuesta H J, Boligan M, Orsaria M G. Int. J. Mod. Phys. D, 2005, **14**: 1959
- 13 Pérez Martínez A, Pérez Rojas H, Mosquera Cuesta H J, Orsaria M G. Int. J. Mod. Phys. D, 2007, **16**: 255
- 14 Chaichian M, Masood S S, Montonen C, Pérez Martínez A, Pérez Rojas H. Phys. Rev. Lett., 2000, **84**: 5261
- 15 Pérez Martínez A, Pérez Rojas H, Mosquera Cuesta H J. Eur. Phys. J. C, 2003, **29**: 111
- 16 González Felipe R, Mosquera Cuesta H J, Pérez Martínez A, Pérez Rojas H. Chin. J. Astron. Astronophys., 2005, **5**: 399
- 17 Ebert D, Klimenko K G. Nucl. Phys. A, 2003, **728**: 203
- 18 Frolov I E, Zhukovsky V C, Klimenko K G. Phys. Rev. D, 2010, **82**: 076002
- 19 Fayazbakhsh S, Sadooghi N. Phys. Rev. D, 2011, **83**: 025026
- 20 Menezes D P, Benghi Pinto M, Avancini S S, Providência C. Phys. Rev. C, 2009, **80**: 065805
- 21 Avancini S. S, Menezes D P, Providência C. Phys. Rev. C, 2011, **83**: 065805; Rabhi A, Providência C. Phys. Rev. C, 2011, **83**: 055801
- 22 Mizher A J, Chernodub M N, Fraga E S. Phys. Rev. D, 2010, **82**: 105016
- 23 Walecka J D. Oxford Stud. Nucl. Phys., 1995, **16**: 1
- 24 Henley E M, Müther H. Nucl. Phys. A, 1990, **513**: 667
- 25 Brown G E, Rho M. Phys. Rev. Lett., 1991, **66**: 2720
- 26 Cohen T D, Furnstahl R J, Griegel D K. Phys. Rev. Lett., 1991, **67**: 961; Phys. Rev. C, 1992, **45**: 1881
- 27 Schertler K, Greiner C, Thoma M H. Nucl. Phys. A, 1997, **616**: 659
- 28 Buballa M, Oertel M. Phys. Lett. B, 1999, **457**: 261
- 29 WEN X J, SU S Z, YANG D H, PENG G X. Phys. Rev. D, 2012, **86**: 034006
- 30 Fowler G N, Raha S, Weiner R M. Z. Phys. C, 1981, **9**: 271
- 31 Chakrabarty S, Raha S, Sinha B. Phys. Lett. B, 1989, **229**: 113
- 32 Chakrabarty S. Phys. Rev. D, 1991, **43**: 627
- 33 Chakrabarty S. Phys. Rev. D, 1993, **48**: 627
- 34 PENG G X, Chiang H C, YANG J J, LI L, LIU B. Phys. Rev. C, 1999, **61**: 015201
- 35 PENG G X, Chiang H C, ZHOU B S, NING P Z, LUO S J. Phys. Rev. C, 2000, **62**: 025801
- 36 WEN X J, ZHONG X H, PENG G X, SHEN P N, NING N Z. Phys. Rev. C, 2005, **72**: 015204
- 37 WANG P. Phys. Rev. C, 2000, **62**: 015204
- 38 PENG G X, NING P Z, Chiang H Q. Phys. Rev. C, 1997, **56**: 491
- 39 ZHENG X P, LIU X W, KANG M, YANG S H. Phys. Rev. C, 2004 **70**: 015803
- 40 Lugones G, Horvath J E., Int. J. Mod. Phys. D, 2003, **12**: 495
- 41 WEN X J, PENG G X, CHEN Y D. J. Phys. G: Nucl. Part. Phys., 2007, **34**: 1697
- 42 WEN X J, PENG G X, SHEN P N. Int. J. mod. Phys. A, 2007, **22**, 1649; PENG G X, WEN X J, CHEN Y D. Phys. Lett. B, 2006, **633**: 313
- 43 YAO W M et al. J. Phys. G: Nucl. Part. Phys., 2006, **33**: 1
- 44 PENG G X, LI A, Lombardo U. Phys. Rev. C, 2008, **77**: 065807
- 45 Laudau L D, Lifshitz E M. Quantum Mechanics. New York: Pergamon, 1965
- 46 Benvenuto O G, Horvath J E, Vucetich H. Int. J. Mod. Phys. A, 1991, **6**: 4769; Alcock C, Olinto A. Annu. Rev. Nucl. Part. Sci., 1988, **38**: 161
- 47 Isayev A A, YANG J. J. Phys. G: Nucl. Part. Sci., 2013, **40**: 035105
- 48 Flipe R G, Martinez A P, Pojas H P, Orsaria. Phys. Rev. C, 2008, **77**: 015807
- 49 Demorest P, Pennucci T, Ransom S, Roberts M, Hessels J. Nature (London), 2010, **467**: 1081
- 50 Antoniadis J et al. Science, 2013, **340**: 1233232
- 51 PENG G X. Nucl. Phys. A, 2005, **747**: 25